High-sensitivity Acoustic Impedance Sensing Using Forward Brillouin Scattering in Highly Nonlinear Fiber

Keyan Zeng, Liang Wang,* Ming Tang, and Deming Liu

National Engineering Laboratory for Next Generation Internet Access System, School of Optics and Electronic Information & Wuhan National Lab for Optoelectronics (WNLO), Huazhong University of Science and Technology, Wuhan 430074, China

**E-mail:* hustwl@hust.edu.cn

Abstract: High-sensitivity acoustic impedance sensing has been demonstrated for the first time by using radial acoustic modes induced forward Brillouin scattering in a highly nonlinear fiber. The measurement sensitivity has been improved to be $3.83\mathrm{MHz}/[\mathrm{kg}/(\mathrm{s}\cdot\mathrm{mm}^2)]$.

1. Introduction

Optical fiber sensors based on backward Brillouin scattering (BBS) have attracted widespread attention due to its capability of distributed temperature and strain sensing [1]. However, BBS based fiber sensors cannot detect the surrounding environment outside the fiber since the light is confined inside the fiber core. In order to distinguish the substance outside the fiber, it usually requires special fiber structures, such as photonic crystal fiber (PCF) [2] and micro-cell cavities [3], which are expensive and complicated for large-scale applications. On the other hand, forward Brillouin scattering (FBS), also regarded as guided acoustic wave Brillouin scattering (GAWBS) [4], is an opto-mechanical effect based on the transverse acoustic wave along the radial direction of the fiber, which makes it possible to detect the surroudning environment outside the fiber [5].

The detection of the external substance is usually achieved by measuring its acoustic impedance. Recently FBS based fiber sensors have been proved to achieve multipoint acoustic impedance sensing [6], simultaneous measurement of temperature and acoustic impedance (sensitivity of $1.3\mathrm{MHz}/[\mathrm{kg}/(\mathrm{s}\cdot\mathrm{mm}^2)]$ by radial acoustic modes $R_{0,m}$ in large effective area fiber) [7] and distributed acoustic impedance sensing (sensitivity of $2.40\mathrm{MHz}/[\mathrm{kg}/(\mathrm{s}\cdot\mathrm{mm}^2)]$ by $R_{0,m}$ in standard single mode fiber, SSMF) [8-10]. However, in the above works, the sensing fiber has small FBS gain, resulting in low signal-to-noise ratio (SNR) and measurement sensitivity. Highly nonlinear fiber (HNLF) is reported to have larger FBS gain [11], and its sensitivity by torsional-radial acoustic modes $TR_{2,m}$ is $0.98\,\mathrm{MHz}/[\mathrm{kg}/(\mathrm{s}\cdot\mathrm{mm}^2)]$ [12], which is still low due to the weak response of $TR_{2,m}$ modes. In this paper, we propose and demonstrate acoustic impedance sensing with high sensitivity by using $R_{0,m}$ modes in an uncoated HNLF, and the measurement sensitivity is improved to be $3.83\mathrm{MHz}/[\mathrm{kg}/(\mathrm{s}\cdot\mathrm{mm}^2)]$.

2. Principle and simulation

Like BBS, the FBS spectrum also shows a Lorentzian line shape, which can be expressed by:

$$g(\Omega) = \frac{g_{0(m)}(\Gamma_m/2)^2}{(\Gamma_m/2)^2 + (\Omega - \Omega_m)^2} \tag{1}$$

where the subscript m refers to the m^{th} order acoustic mode. $g_{0(m)}$ is the gain coefficient, Γ_m is the linewidth and Ω_m is the center frequency of the m^{th} order acoustic resonance. Two kinds of transverse acoustic waves are usually involved due to the circular symmetry of the fiber [4]: the radial-mode acoustic wave ($R_{0,m}$) and torsional-radial mode acoustic wave ($TR_{2,m}$). Here, we choose $R_{0,m}$ modes induced FBS spectrum for sensing due to its strong response and hence high measurement sensitivity when compared with $TR_{2,m}$ modes. The linewidth of the FBS spectrum Γ_m is related to the acoustic reflectivity r, which can reflect the acoustic loss between the cladding and the environment outside the fiber. For $R_{0,m}$ modes, Γ_m is determined by [6]:

$$\Gamma_m = \Gamma_{int} + \frac{V_d}{2\pi a} ln\frac{1}{|r|}, \qquad |r| = |Z_f - Z_0|/(Z_f + Z_0) \tag{2}$$

where V_d is the longitudinal acoustic wave velocity, a is the radius of the fiber cladding, Γ_{int} is the intrinsic linewidth of the acoustic modes and the reflectivity r is dependent on the acoustic impedance of the fiber cladding Z_f and the environment Z_0. As a result, when the external environment changes, it will cause the change of Γ_m. By measuring the linewidth, the acoustic impedance of the external environment can be detected. Obviously, it is expected to have larger FBS gain for better measurement sensitivity. The gain coefficient $g_{0(m)}$ in Eq. (1) can be expressed by [11]:

$$g_{0(m)} = \frac{\omega_0 \gamma_e^2 \left|Q_{0(m)} Q_{1(m)}\right|}{2n_{eff}^2 c^2 \rho_0 \Omega_m \Gamma_m} \tag{3}$$

where ω_0 is the frequency of the optical wave, γ_e is the electrostrictive constant, n_{eff} is the effective refractive index, c is the speed of the light, ρ_0 is the density of the silica, $Q_{0(m)}$ and $Q_{1(m)}$ are the acousto-optic coupling coefficient which can be determined by $Q_{0(m)} = \langle E_0^2, \rho_{0m} \rangle$ and $Q_{1(m)} = \langle \nabla_\perp^2 E_0^2, \rho_{0m} \rangle$. E_0 is the normalized optical mode and can be approximated by $E_0(\mathrm{r}) \approx \exp[-(r/\omega)^2]/(\pi\omega^2)$, where ω is the effective mode radius. Based on Eq. (3), we calculate the normalized gain coefficient for $R_{0,m}$ modes in HNLF and compare it with that in SSMF. According to the fiber datasheet, we set $\omega = 1.65\mu m$ for HNLF and $\omega = 4\mu m$ for SSMF. The results are shown in Fig. 1(a)-(d). Due to the high acousto-optical coupling efficiency, the gain coefficient in HNLF reaches maximum of 1.0 at $R_{0,21}$ mode whose center frequency is 995MHz. For HNLF, the gain coefficient still maintains above 0.5 even if the center frequency of the FBS spectrum reaches 1.5GHz. While for SSMF, the maximum gain coefficient is only 0.41 at $R_{0,9}$ mode whose center frequency is 419MHz, as shown in Fig. 1(c). Fig. 1(b) and (d) show the FBS spectrum of $R_{0,21}$ in HNLF and $R_{0,9}$ in SSMF, respectively. We can see that HNLF has larger FBS gain than that of SSMF, which is helpful to achieve high sensitivity for acoustic impedance sensing.

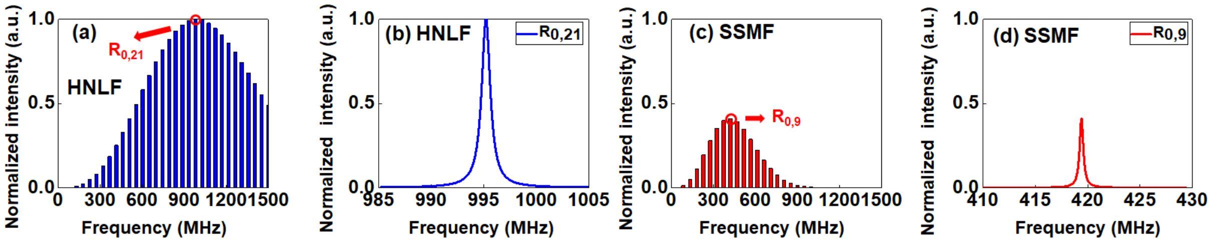

Fig. 1 Normalized gain coefficient for $R_{0,m}$ modes in (a) HNLF and (c) SSMF; FBS spectrum by (b) $R_{0,21}$ in HNLF and (d) $R_{0,9}$ in SSMF.

3. Experiment and results

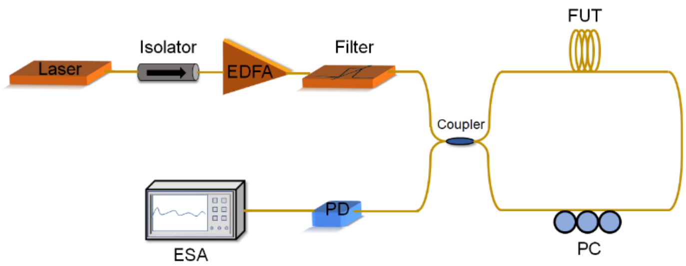

Fig. 2 Experimental setup for acoustic impedance sensing using FBS in HNLF. EDFA: erbium-doped fiber amplifier; PC: polarization controller; FUT: fiber under test; PD: photodetector. ESA: electrical spectrum analyzer.

The experimental setup is shown in Fig. 2. We employ a fiber Sagnac loop to measure the $R_{0,m}$ modes induced FBS spectrum. The output of the laser at 1550.12 nm is amplified by an erbium-doped fiber amplifier (EDFA). The amplified spontaneous emission (ASE) noise is eliminated by a bandpass filter. The light with ~20dBm power is directed to the Sagnac loop which consists of a 50:50 coupler, a fiber under test (FUT) and a polarization controller (PC). By adjusting the PC, the $R_{0,m}$ modes are stimulated and $TR_{2,m}$ modes are suppressed, and the phase modulation induced by the $R_{0,m}$ modes is converted to intensity modulation when the counter-propagating optical waves interfere at the coupler. The output beat signal is detected by using a 1.5GHz photodetector (PD) and is then analyzed on an electrical spectrum analyzer (ESA).

A 10m-long uncoated HNLF as the FUT is immersed into the sucrose solution with different concentrations. In the experiment, we choose the FBS spectrum induced by $R_{0,20}$ mode for the demonstration since it can be easily collected without the overlap of other $TR_{2,m}$ modes. Note $R_{0,20}$ mode still has almost the maximum gain

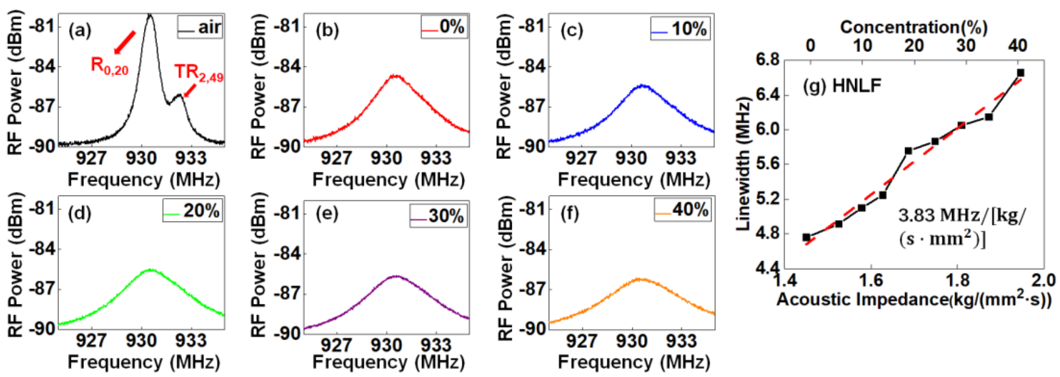

Fig. 3 Measured $R_{0,20}$ induced FBS spectrum in HNLF for different external environment (a) air, (b) 0%, (c) 10%, (d) 20%, (e) 30%, (f) 40% concentrations of the sucrose solution; (g) linewidth of the $R_{0,20}$ induced FBS spectrum versus acoustic impedance.

coefficient according to Fig. 1. The results are shown in Fig. 3(a)-(f). For comparison, we also measure the FBS spectrum when the HNLF is placed in air, as shown in Fig. 3(a) where the small peak is due to the incomplete suppression of the $TR_{2,49}$ mode. Lorentzian curve fitting is carried out and the linewidth is measured to be 1.60MHz for the air and 4.76, 5.01, 5.76, 6.05, 6.66MHz for 0-40% concentrations (10% step) of the sucrose solution, respectively. The center frequency of the $R_{0,20}$ mode induced FBS spectrum is 930.7MHz. Fig. 3(g) plots the relationship between the measured linewidth and the acoustic impedance of the sucrose solution. The acoustic impedance of the sucrose solution is linearly dependent on its concentration [7]. By linear fitting, the measurement sensitivity is calculated to be $3.83\mathrm{MHz}/[\mathrm{kg}/(\mathrm{s}\cdot\mathrm{mm}^2)]$, as illustrated by the slope of the red dash line in Fig. 3(g). As a contrast, a 10m-long uncoated SSMF is used as the FUT and the same procedure is performed except $R_{0,9}$ mode is measured due to its largest gain coefficient in SSMF. The EDFA output is adjusted to ensure that the optical power after passing through SSMF is consistent with the case of HNLF for fair comparison. The FBS spectra for different environment are shown in Fig. 4(a)-(f). The linewidth is calculated to be 0.60MHz for the air and 4.03, 4.40, 4.74, 5.00, 5.43MHz for 0-40% concentrations (10% step) of the sucrose solution, respectively. The center frequency for $R_{0,9}$ mode in SSMF is 417.8MHz. The sensitivity using SSMF is calculated to be $2.70\mathrm{MHz}/[\mathrm{kg}/(\mathrm{s}\cdot\mathrm{mm}^2)]$, as shown in Fig. 4(g). By comparing Fig 3(g) with Fig. 4(g), it can be seen that the sensitivity of acoustic impedance sensing using HNLF is larger than that using SSMF.

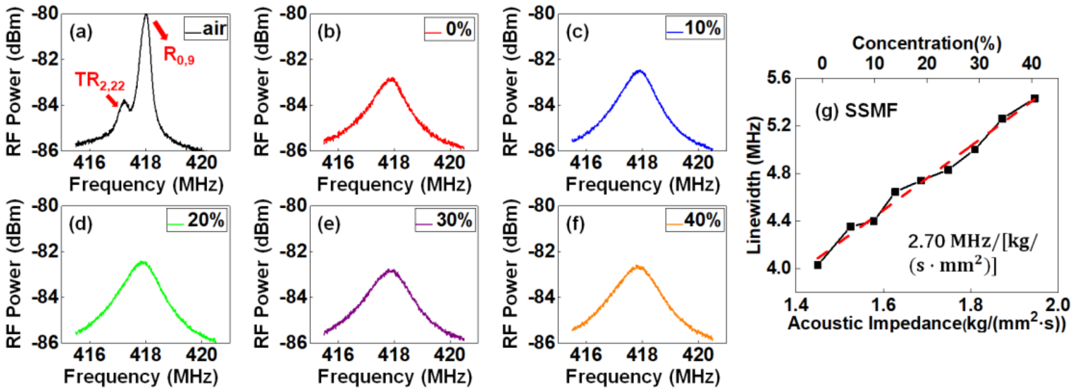

Fig. 4 Measured $R_{0,9}$ induced FBS spectrum in SSMF for different external environment (a) air, (b) 0%, (c) 10%, (d) 20%, (e) 30%, (f) 40% concentrations of the sucrose solution; (g) linewidth of $R_{0,9}$ induced FBS spectrum versus the acoustic impedance.

4. Conclusion

We have demonstrated high-sensitivity acoustic impedance sensing by using strong $R_{0,20}$ mode induced FBS in the HNLF. Due to the high acousto-optical coupling efficiency, HNLF has larger FBS gain than SSMF, giving rise to better SNR and sensitivity, especially at high frequency range. The measurement sensitivity using HNLF is improved to be $3.83\,\mathrm{MHz}/[\mathrm{kg}/(\mathrm{s}\cdot\mathrm{mm}^2)]$, compared with $2.70\,\mathrm{MHz}/[\mathrm{kg}/(\mathrm{s}\cdot\mathrm{mm}^2)]$ of using SSMF. The improved acoustic impedance sensitivity together with excellent temperature sensitivity of FBS at high frequency range can enhance simultaneous measurement of the acoustic impedance and temperature in the future.

Acknowledgment

National Natural Science Foundation of China (62005087), Science Foundation of Donghai Laboratory (DH-2022KF01015).

References

[1] X. Bao & L. Chen, "Recent progress in Brillouin scattering based fiber sensors," Sensors. **11**, 4152-4187 (2011)
[2] I. Dicaire, A. Rossi, S. Combrié, & L. Thévenaz, "Probing molecular absorption under slow-light propagation using a photonic crystal waveguide," Opt. Lett. **37**, 4934-4936 (2012).
[3] E. Preter, B. Preloznik, V. Artel, C. Sukenik, D. Donlagic, & A. Zadok, "Monitoring the Evaporation of Fluids from Fiber-Optic Micro-Cell Cavities, " Sensors **13**, 15261-15273 (2013).
[4] R. Shelby, M. Levenson, & P. Bayer, "Guided acoustic-wave brillouin scattering". physical review b condensed matter, **31**, 5244 (1985).
[5] Y. Antman, A. Clain, Y. London, & A. Zadok, "Optomechanical sensing of liquids outside standard fibers using forward stimulated Brillouin scattering," Optica **3**, 510-516 (2016).
[6] Z. Zheng, Z. Li, X. Fu, L. Wang, & H. Wang, "Multipoint acoustic impedance sensing based on frequency-division multiplexed forward stimulated Brillouin scattering," Opt. Lett, **45**, 4523-4526, (2020).
[7] Z. Zhang, Y. Lu, J. Peng, & Z. Ji, "Simultaneous measurement of temperature and acoustic impedance based on forward Brillouin scattering in LEAF," Opt. Lett, **46**, 1776-1779 (2021).
[8] G. Bashan,H. Diamandi, Y. London & E. Preter "Optomechanical time-domain reflectometry", Nature communications, **9**, 1-9 (2018).
[9] Chow, D. M., Zhisheng, Y., Soto, M. A., & Thévenaz Luc, " Distributed forward brillouin sensor based on local light phase recovery", Nature Communications, **9**, 2990 (2018).
[10] C. Pang, Z. Hua, D. Zhou, H. Zhang, L. Chen, X. Bao, & Y. Dong, "Opto-mechanical time-domain analysis based on coherent forward stimulated Brillouin scattering probing," Optica **7**, 176-184 (2020).
[11] J. Wang, Y. Zhu & R. Zhang, "FSBS resonances observed in a standard highly nonlinear fiber", Optics Express, **19**, 5339–5349, (2011).
[12] N. Hayashi & S. Yamashita, "Observation of depolarized guided acoustic-wave Brillouin scattering in partially uncoated optical fibers", Japanese Journal of Applied Physics, **57**, 020307, (2018).